

Advanced-Retarded Differential Equations in Quantum Photonic Systems

Unai Alvarez-Rodriguez,^{1,*} Armando Perez-Leija,^{2,3} Iñigo L. Egusquiza,⁴ Markus Gräfe,² Mikel Sanz,¹ Lucas Lamata,¹ Alexander Szameit,² and Enrique Solano^{1,5}

¹*Department of Physical Chemistry, University of the Basque Country UPV/EHU, Apartado 644, 48080 Bilbao, Spain*

²*Institute of Applied Physics, Abbe Center of Photonics,*

Friedrich-Schiller-Universität Jena, Max-Wien-Platz 1, Jena 07743, Germany

³*Max Born Institute, Max Born Strasse 2A, 12489 Berlin, Germany*

⁴*Department of Theoretical Physics and History of Science,*

University of the Basque Country UPV/EHU, Apartado 644, 48080 Bilbao, Spain

⁵*IKERBASQUE, Basque Foundation for Science, Maria Diaz de Haro 3, 48013 Bilbao, Spain*

(Dated: July 22, 2022)

We propose the realization of photonic circuits whose dynamics is governed by advanced-retarded differential equations. Beyond their mathematical interest, these photonic configurations enable the implementation of quantum feedback and feedforward without requiring any intermediate measurement. We show how this protocol can be applied to implement positive and negative delay effects in the classical and quantum realms. Our results elucidate the potential of the protocol as a promising route towards integrated quantum control systems on a chip.

In advanced-retarded (A-R) differential equations, also known as mixed functional differential equations, the derivative of the associated function explicitly depends on itself evaluated at different advanced-retarded values of the *time variable* [1–5]. In order to solve such A-R equations either analytically or numerically, we require the knowledge of the solution history out of the domain of the equation. In many scientific disciplines A-R differential equations are used to describe phenomena containing feedback and feedforward interactions in their evolution [6–8]. In physics, for instance, A-R equations can be used to model systems exhibiting *temporal symmetries* in the evolution. As a prominent example one may mention the application of A-R equations [9] in Wheeler-Feynman absorber theory [10, 11].

In the context of quantum mechanics, the implementation of feedback is more intricate than in the classical case due to the sensitivity of quantum systems to measurements. In this regard, a set of techniques has been developed for the realization of feedback-dependent systems, each of them employing different resources such as dynamical delays [12, 13], machine learning optimization [14], weak measurements [15, 16], including quantum memristors [17, 18], and projective measurements for digital feedback [19] among others. Certainly, the inclusion of feedback or memory effects in quantum dynamical systems has extended the scope of quantum protocols, and it has allowed for the study and reproduction of more complex phenomena. Therefore, devising schemes for engineering Hamiltonians that display advanced-retarded dynamics is of great relevance. Along these lines, the field of non-Markovian quantum dynamics focuses on the study of effective equations that govern the evolution of systems interacting with state-dependent environments [20–23]. As a result, estimation of non-Markovianity sheds light on the memory content of the systems under study.

In this letter, we show that photonic lattices can be

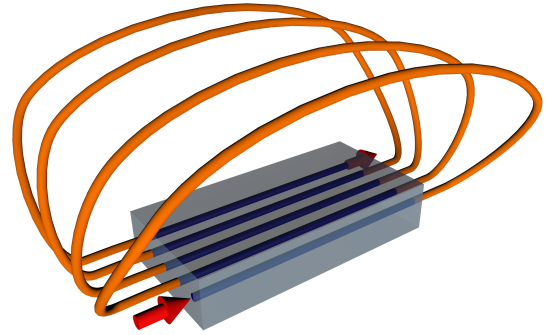


FIG. 1: Illustration of the chip for implementing the photonic simulator in Eq. (2), where the arrows represent the input and output ports, while the lines inside and outside the chip represent the waveguides and fiber connections, respectively.

used to effectively tailor the dynamics of classical and quantum light fields in an advanced-retarded fashion. Our strategy is to exploit the duality between light propagation in space and time. More specifically, we use the existing mapping between time and the propagation coordinate [24]. Our A-R photonic approach utilises the isomorphism existing between the steady state of judiciously designed photonic waveguide circuits and solutions of A-R differential equations. We foresee that the inherent versatility of the proposed system will make the implementation of feedback and feedforward noticeably simple, in both classical and quantum frameworks, and thus may open the door to many interesting applications in integrated quantum technologies.

To introduce our protocol, we start by considering the following first-order linear and non-autonomous A-R differential equation [1]

$$i \frac{dx(t)}{dt} = \beta(t)x(t) + \kappa^-(t)x(t - \tau) + \kappa^+(t)x(t + \tau), \quad (1)$$

with $\kappa^+(t) = \kappa^-(t + \tau)$, and boundary conditions $\kappa^-(0 < t < \tau) = \kappa^+((N - 1)\tau < t < N\tau) = 0$. We associate the functions $x(t)$, $x(t \pm \tau)$ with the mode amplitude of classical monochromatic waves traversing the j -th and $j \pm 1$ -th waveguides, $a_j(z)$ and $a_{j \pm 1}(z)$, of an array of N evanescently coupled waveguides, each supporting a single mode and having a *time-dependent* propagation constant $\beta(z)$. This system is governed by a set of N differential equations [25]

$$i \frac{da_j}{dz} = \beta(z)a_j(z) + \kappa_{j,j+1}(z)a_{j+1}(z) + \kappa_{j,j-1}(z)a_{j-1}(z), \quad (2)$$

with $j \in [1, N]$. In quantum optics, the dynamics of single photons traversing this type of devices is modeled with a set of Heisenberg equations isomorphic to Eq. (2), which are achieved by replacing the classical mode amplitudes a_j by the corresponding annihilation bosonic operators \hat{a}_j [26, 27]. In order to make Eq. (2) isomorphic to Eq. (1), we must impose a continuity condition $a_j(0) = a_{j-1}(\tau)$ within the interval $j \in [2, N - 1]$. Physically, this condition implies that the mode field a_{j-1} , at the propagation distance of $(j - 1)\tau$ (τ being the length of the waveguides), has to be fed back into the input of the j -th waveguide. Furthermore, the finiteness of the waveguide array imposes the boundary conditions $\kappa_{1,0} = \kappa_{N,N+1} = 0$. Additionally, we establish the aforementioned mapping of the independent variable t into the spatial coordinate z . Therefore, our protocol requires the implementation of waveguide lattices endowed with input-output connections as illustrated in Fig. 1.

Physically, the initial condition $a_1(0)$ is implemented by continuously injecting light into the system. This condition is crucial to establish the isomorphism between the light dynamics in the waveguide array and the solution of Eq. (1). As a result, this solution is obtained in the stationary regime of our photonic system. Once the intensity is measured, the modulus square of the solution is obtained by joining the intensity evolution of each waveguide in a single variable. See Fig. 2 for a demonstration of the potentiality of our protocol, where we analyze the setup depicted in Fig. 1 with $N = 6$ and constant lattice parameters, $\beta(z) = 1$, $\kappa = \sqrt{\beta + N}$ and $\tau = 1$. The light dynamics occurring in such an array is governed by Eq. (2).

An interesting point to highlight here is the existence of a z reversal symmetry in the simulation with respect to the central point of the evolution, $z_c = N\tau/2$, for constant lattice parameters. This relation holds for the modulus square of the solution, $aa^*(z_c + z) = aa^*(z_c - z)$. Consequently, after the system reaches the steady state, it simultaneously fulfills the periodic boundary condition, $a(0) = a(N\tau)$, where we have neglected a global phase factor. This property combined with the space-time analogy open a possible framework for the study and implementation of closed timelike curve (CTC) gates [28–30].

Another interesting scenario arises when considering

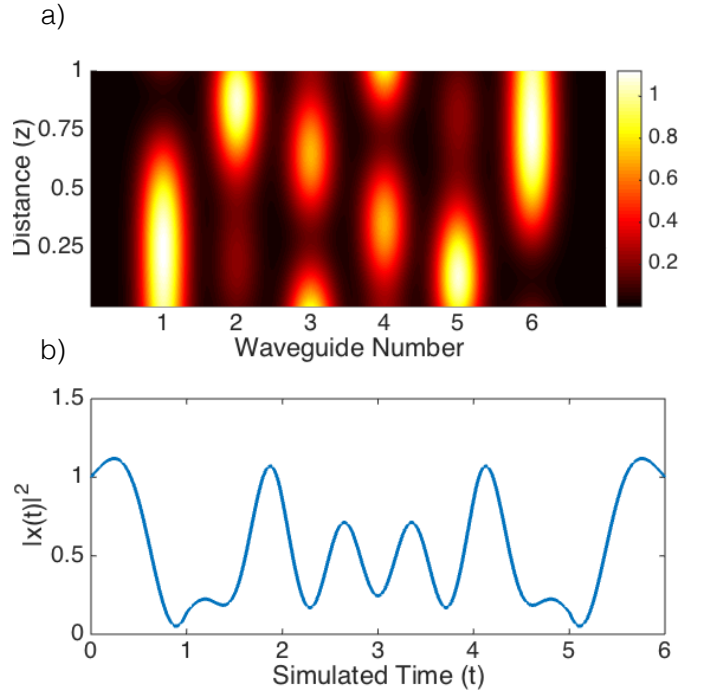


FIG. 2: (a) Intensity evolution for an array having $N = 6$ waveguides and constant lattice parameters $\beta = 1$, $\kappa = \sqrt{\beta + N}$ and $\tau = 1$. (b) Intensity of all the waveguides concatenated in a single curve, which represents the absolute square of the solution of Eq. (2).

space dependent parameters in Eq. (2), which in the context of photonic lattices means that the system acquires dynamics. The dynamical character is achieved with modulations of the refractive index of individual waveguides. We consider an implementable system conformed by a periodic variation $\beta(z) = \beta_0 + \epsilon \cos(\omega z)$, where β_0 is a constant, ϵ is the modulation amplitude, and ω stands for the modulation frequency along z . For illustration purposes, we provide a numerical calculation of this photonics simulator in the Supplemental Material [31]. Notice that in the context of advanced-retarded equations the time dependence allows us to encode non-autonomous equations, which are hard to compute in general.

We now turn our attention to demonstrate how our protocol can be extended to provide solutions of systems of classical and quantum A-R equations. To this end, we encode every unknown function in a waveguide array, and place all the involved arrays close to each other in such a way that light fields traversing the system can tunnel from array to array. In this manner, all the functions are self-coupled and coupled to others, enriching the dynamics of the systems. In order to explain the operation principle of the protocol, we focus on the simplest case of two variables. Note that in this case, we can relate each array x and y to a component of a qubit, $|\psi\rangle = (a_x, a_y)^T$,

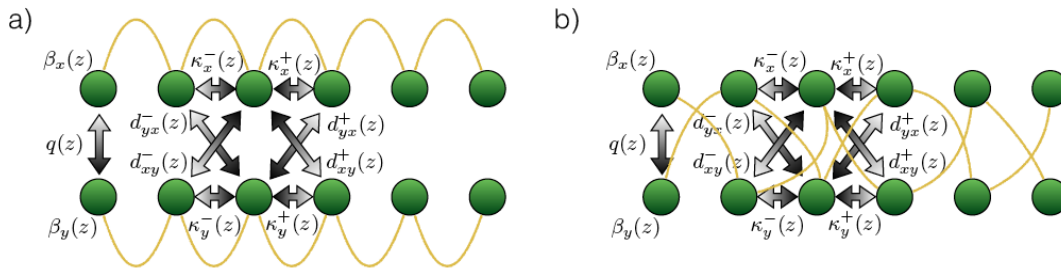


FIG. 3: Front side view of the chip showing the input-output connections and the parameters of the simulation. Here β is the propagation constant, q is the vertical coupling constant, κ is the horizontal coupling constant and d the diagonal coupling constant. a) The scheme in which each plane is associated with a component of the qubit simulates Eq. (3). b) The crossed links allow for a stronger temporal mixing of the qubit components in the derivative. This situation corresponds to the second example of Eq. (3).

where T denotes the transpose. Thereby, we mold its dynamics to evolve according to an effective A-R differential equation. As a first possibility, we can put together two lattices in which the feedback takes place as depicted in Fig. 3a. In this scenario, the light can hop to its neighboring sites as well as to the sites of the adjacent array. This arrangement enables the time evolution simulation of a single qubit Hamiltonian combined with two terms corresponding to advanced and retarded couplings

$$i|\dot{\psi}(t)\rangle = H(t)|\psi(t)\rangle + H^+(t)|\psi(t+\tau)\rangle + H^-(t)|\psi(t-\tau)\rangle, \quad (3)$$

$$H(t) = \begin{pmatrix} \beta_x(t) & q(t) \\ q(t) & \beta_y(t) \end{pmatrix}, H^+(t) = \begin{pmatrix} \kappa_x^+(t) & d_{xy}^+(t) \\ d_{yx}^+(t) & \kappa_y^+(t) \end{pmatrix}, \\ H^-(t) = \begin{pmatrix} \kappa_x^-(t) & d_{xy}^-(t) \\ d_{yx}^-(t) & \kappa_y^-(t) \end{pmatrix}. \quad (4)$$

A second configuration arises by mixing the connectors as shown in Fig. 3b. In this case, we flip the qubit in the advanced and retarded times. Even though the equation exhibits the same structure as Eq. (3), the forward and backward Hamiltonians, H^+ and H^- are the same matrices given in Eq. (4) multiplied on the left by σ_x . Here $H(t)$, $H^+(t)$, and $H^-(t)$ depend on the parameter β and on the coupling between waveguides belonging to different arrays and the coupling between the guides of the same array. The vertical coupling is referred to as q , while the transverse coupling constants are represented by κ and the labels (x, y) correspond to each plane where the arrays are located. Moreover, d accounts for the diagonal coupling. In addition to the conditions for each array in Eq. (1), the following consistency and boundary conditions are fulfilled,

$$H^+((n-1)\tau < t < n\tau) = H^-(0 < t < \tau) = 0, \\ d_{yx}^+(t) = d_{xy}^-(t + \delta), \quad d_{xy}^+(t) = d_{yx}^-(t + \delta). \quad (5)$$

In the Supplemental Material [31], a numerical calculation of Eq. (3) is provided.

We next consider a variant of Eq. (1) with multiple delays. This configuration arises when we allow each waveguide to couple to multiple neighbors and after reordering the feedback connectors. The first non-trivial example is a two-time A-R equation

$$i\dot{x}(t) = \beta(t)x(t) + \kappa^+(t)x(t+\tau) + \kappa^{++}(t)x(t+2\tau) \\ + \kappa^-(t)x(t-\tau) + \kappa^{--}(t)x(t-2\tau). \quad (6)$$

Experimentally, the arrangement can be engineered by fabricating the waveguides in a zig-zag configuration. The resulting equation shares the structure of an A-R differential advanced-retarded with additional feedback and feedforward terms. For this particular system, the coupling coefficients are related as

$$k^{++}(t) = k^{--}(t+2\tau), \quad k^+(t) = k^-(t+\tau), \quad (7)$$

with the appropriate boundary conditions. See the Supplemental Material [31] for a simulation of Eq. (6).

One last generalization of the A-R simulator consists in introducing complex dynamical parameters. This can be achieved by combining our feedback technique with Bloch oscillator lattices [32–34]. These types of arrays can be implemented by including a transverse ramping on the potential of the waveguides or by curving the waveguide arrays. Provided the evolution equations for the Bloch oscillator array, $ia_n + n\beta za_n + \kappa^+ a_{n+1} + \kappa^- a_{n-1} = 0$, and making the formal transformation $a_n = \tilde{a}_n(z) \exp(in\phi(z))$, with $\phi(z) = \int_0^z \beta(z') dz'$, one can show that it is formally equivalent to a system endowed with complex coefficients, $i\tilde{a}_n + \exp(in\phi(z))\kappa^+ \tilde{a}_{n+1} + \exp(-in\phi(z))\kappa^- \tilde{a}_{n-1}$. The inclusion of arbitrary complex parameters could be used to enhance the versatility of the protocol. Furthermore, a complete control of the coupling constants would allow to simulate higher-order equations via systems of first-order equations.

Even though the toolbox we present here is valid for simulating diverse physical configurations, it can be generalized by an appropriate mathematical treatment. Let

$M(t)$ be the matrix containing the information about the propagation constant and couplings among the waveguides defined by $i\dot{a}(t) = M(t)a(t)$, F the matrix encoding the input-output connections, and α the initial state independent of the feedback and feedforward mechanism, such that $a(0) = Fa(\tau) + \alpha$. Consider now that the dynamical equation is solvable in terms of the evolution operator $U(t)$, $a(t) = U(t)a(0)$. Our goal is to determine the complete initial condition $a(0)$ in terms of the independent initial condition α , evolution operator $U(t)$ and input-output matrix F . The consistency relations at $a(\tau)$ impose that $a(0)$ has to fulfill, $a(\tau) = U(\tau)a(0)$,

$$\begin{aligned} a(0) &= Fa(\tau) + \alpha \Rightarrow a(0) = (\mathbb{1} - FU(\tau))^{-1} \alpha, \\ a(t) &= U(t)(\mathbb{1} - FU(\tau))^{-1} \alpha. \end{aligned} \quad (8)$$

Notice that this relation holds for any α , allowing the input of quantum states superposed in more than one waveguide, and is also valid for different configurations of couplings U and connections F , limited by the existence of the inverse of $(\mathbb{1} - FU(\tau))$. Moreover, we can think of different experimental conditions in which the connections happen at distinct evolution times τ_i , $a(0) = \sum_i F_i a(\tau_i) + \alpha$, resulting in $a(t) = U(t)(\mathbb{1} - \sum_i F_i U(\tau_i))^{-1} \alpha$.

At this point the protocol enables to implement systems of multiple delay advanced-retarded differential equation of first or higher orders, therefore allowing to address several applications in fields as physiology, economy and neuroscience [6–8]. In the remainder, in order to make the algorithm realistic, we analyze the main limitations of the protocol regarding its interpretation and experimental realization.

If we interpret the solution of the qubit equation, Eq. (3), as a quantum particle we obtain a particle whose probability is not always normalized, associated with the forward and backward jumps of the particle. Although this effect excludes in principle the particle interpretation, absorbing potentials [35] account for this kind of kinematics. Moreover, the solution can always be divided by a constant, and the advanced-retarded equation will still be fulfilled. We can then calculate the non-Markovianity measurement, and see that quantum memory effects are present in the time evolution.

An important source of errors is given by the decoherence of the quantum state in the time elapsed until the equilibrium situation in the system is achieved. This time is related with the population in the equilibrium situation, which is unknown before the experiment is realized. Identifying the relation between the resonances and the dynamical parameters could be helpful for estimating the population in the stationary state, and therefore the total experimental time for achieving this state. See Fig. 4 for an scheme of the error depending on the distance from the stationary state. Another possible approach is to employ the analogy explained in Fig. 4 for obtaining

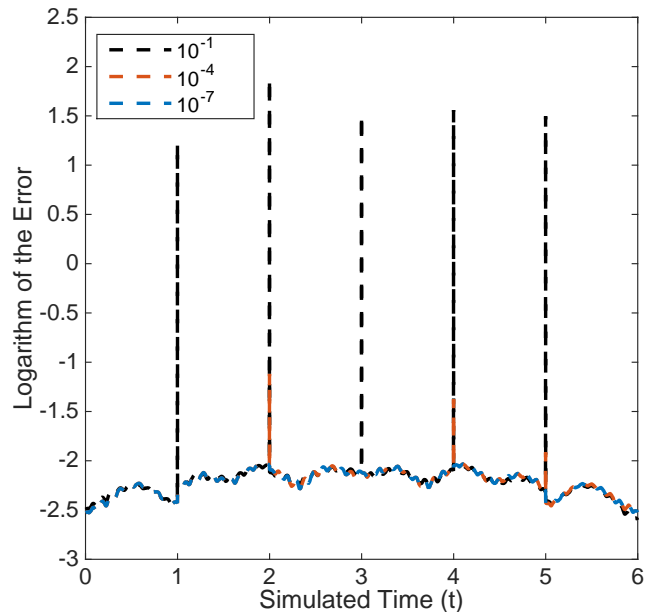


FIG. 4: We depict the decimal logarithm of the error as a function of time for three runs of the simulation with different distances with respect to the stationary state. The fact that the effective interaction between photons is zero makes possible the analogy between the stationary state solution and the accumulation of solutions for an initial excitation combined until the initial population has escaped from the output port. Therefore, the distance is calculated as the norm of the population that remains in the chip. The dynamical constants of the system are equivalent to the ones in Fig. 2.

the complete solution as a combination of snapshots of the chip at different times. This is specially useful in the quantum case, because it allows to implement the experiment using a single photon instead of a constant supply of energy. While both methods provide the solution to the advanced-retarded differential equation, only the stationary state technique allows to obtain the physical state of the system at $t = n\tau$, which has the same norm as the initial state in $t = 0$.

We have to take into account the losses introduced by the fiber connections that will break the continuity condition allowing us to simulate Eq. (1) in terms of Eq. (2). The length and propagation constant of these fibers have to be tuned so that no phase is introduced in the evolution. Additionally, the space dependence of propagation and coupling constants is limited by the experimentally realizable functions. The degrees of freedom to consider are the writing precision for modifying the propagation constants and the spatial path of each waveguide for modifying the coupling constants.

In conclusion, we have developed a flexible and realistic toolbox for implementing advanced-retarded differential equations in integrated quantum photonics circuits. We have shown that our analogy enables the simulation of time-dependent systems of advanced-retarded equations

in the classical and quantum realms, which in the context of quantum information can be employed to realize feedback and feedforward driven dynamics. Therefore, we consider that our work enhances the versatility of quantum simulators in the abstract mathematical direction and in terms of applications for retrospective and prospective quantum memory.

The authors acknowledge support from Spanish MINECO FIS2015-69983-P, Ramón y Cajal Grant RYC-2012-11391, UPV/EHU UFI 11/55 and EHUA14/04, Basque Government BFI-2012-322, the Deutsche Forschungsgemeinschaft (grants SZ 276/7-1, SZ 276/9-1, BL 574/13-1, GRK 2101/1) and the German Ministry for Science and Education (grant 03Z1HN31).

* Electronic address: unaialvarezr@gmail.com

- [1] A. D. Myshkis, *Mixed Functional Differential Equations*, *J. Math. Sci.* **129**, 5 (2005).
- [2] A. Rustichini, *Functional Differential Equations of Mixed Type: The Linear Autonomous Case*, *J. Dyn. Diff. Eq.* **1**, 2 (1989).
- [3] J. Mallet-Paret, *The Fredholm alternative for functional differential equations of mixed type*, *J. Dyn. Diff. Eq.* **11**, 1 (1999).
- [4] L. Berezansky, E. Braverman, and S. Pinelas, *On nonoscillation of mixed advanced-delay differential equations with positive and negative coefficients*, *Comput. Math. Appl.* **58**, 766 (2009).
- [5] N. J. Ford, P. M. Lumb, P. M. Lima, and M. F. Teodoro, *The numerical solution of forward-backward differential equations: Decomposition and related issues*, *J. Comput. Appl. Math.* **234**, 2745 (2010).
- [6] J. C. Lucero, *Advanced-delay differential equation for aeroelastic oscillations in physiology*, *Biophys. Rev. Lett.* **3**, 125 (2008).
- [7] F. Collard, O. Licandro, and L. A. Puc, *The short-run dynamics of optimal growth models with delays*, *Ann. Econ. Stat.* **90**, 127 (2008).
- [8] H. Chi, J. Bell, and B. Hassard, *Numerical solution of a nonlinear advance-delay-differential equation from nerve conduction theory*, *J. Math. Biol.* **24**, 583 (1986).
- [9] L. S. Schulman, *Some differential-difference equations containing both advance and retardation*, *J. Math. Phys.* **15**, 295 (1974).
- [10] J. A. Wheeler and R. P. Feynman, *Interaction with the Absorber as the Mechanism of Radiation*, *Rev. Mod. Phys.* **17**, 157 (1945).
- [11] J. A. Wheeler and R. P. Feynman, *Classical Electrodynamics in Terms of Direct Interparticle Action*, *Rev. Mod. Phys.* **21**, 425 (1949).
- [12] S. Whalen, *Open Quantum Systems with Time-Delayed Interactions*, PhD Thesis, University of Auckland, (2015).
- [13] H. Pichler and P. Zoller, *Photonic Circuits with Time Delays and Quantum Feedback*, *Phys. Rev. Lett.* **116**, 093601 (2016).
- [14] S. Mavadia, V. Frey, J. Sastrawan, S. Dona, and M. J. Biercuk, *Prediction and real-time compensation of qubit decoherence via machine-learning*, arXiv:1604.03991 (2016).
- [15] S. Lloyd and J.-J. E. Slotine, *Quantum feedback with weak measurements*, *Phys. Rev. A* **62**, 012307 (2000).
- [16] G. G. Gillett, R. B. Dalton, B. P. Lanyon, M. P. Almeida, M. Barbieri, G. J. Pryde, J. L. O'Brien, K. J. Resch, S. D. Bartlett, and A. G. White, *Experimental Feedback Control of Quantum Systems Using Weak Measurements*, *Phys. Rev. Lett.* **104**, 080503 (2010).
- [17] P. Pfeiffer, I. L. Egusquiza, M. Di Ventra, M. Sanz, and E. Solano, *Quantum Memristors*, arXiv:1511.02192 (2015).
- [18] J. Salmilehto, F. Deppe, M. Di Ventra, M. Sanz, and E. Solano, *Quantum Memristors with Superconducting Circuits*, arXiv:1603.04487 (2016).
- [19] D. Ristè and L. DiCarlo, *Digital Feedback in Superconducting Quantum Circuits*, arXiv: 1508.01385 (2015).
- [20] H.-P. Breuer, E.-M. Laine, J. Piilo, and B. Vacchini, *Colloquium: Non-Markovian dynamics in open quantum systems*, *Rev. Mod. Phys.* **88**, 021002 (2016).
- [21] A. Rivas, S. F. Huelga, and M. B. Plenio, *Quantum non-Markovianity: characterization, quantification and detection*, *Rep. Prog. Phys.* **77**, 094001 (2014).
- [22] I. de Vega and D. Alonso, *Dynamics of non-Markovian open quantum systems*, arXiv:1511.06994 (2015).
- [23] F. A. Pollock, C. Rodríguez-Rosario, T. Frauenheim, M. Paternostro, and K. Modi, *Complete framework for efficient characterisation of non-Markovian processes*, arXiv:1512.00589 (2015).
- [24] T. Eichelkraut, C. Vetter, A. Perez-Leija, H. Moya-Cessa, D. N. Christodoulides, and A. Szameit, *Coherent random walks in free space*, *Optica* **4**, 268 (2014).
- [25] A. Szameit and S. Nolte, *Discrete optics in femtosecond-laser-written photonic structures*, *J. Phys. B: At., Mol. Opt. Phys.* **43**, 163001 (2010).
- [26] W. K. Lai, V. Bužek, and P. L. Knight, *Nonclassical fields in a linear directional coupler*, *Phys. Rev. A* **43**, 6323 (1991).
- [27] T. Meany, M. Gräfe, R. Heilmann, A. Perez-Leija, S. Gross, M. J. Steel, M. J. Withford, and A. Szameit, *Laser written circuits for quantum photonics*, *Laser Photon. Rev.* **9**, 363 (2015).
- [28] D. Deutsch, *Quantum mechanics near closed timelike lines*, *Phys. Rev. D* **44**, 3197 (1991).
- [29] S. Lloyd, *et al.*, *Closed Timelike Curves via Postselection: Theory and Experimental Test of Consistency*, *Phys. Rev. Lett.* **106**, 040403 (2011).
- [30] M. Ringbauer, M. A. Broome, C. R. Myers, A. G. White, and T. C. Ralph, *Experimental simulation of closed time-like curves*, *Nat. Commun.* **5**, 4145 (2014).
- [31] See Supplemental Material for further details of the protocol.
- [32] G. Lenz, I. Talanina, and C. Martijn de Sterke, *Bloch Oscillations in an Array of Curved Optical Waveguides*, *Phys. Rev. Lett.* **83**, 963 (1999).
- [33] U. Peschel, T. Pertsch, and F. Lederer, *Optical Bloch oscillations in waveguide arrays*, *Opt. Lett.* **23**, 1701 (1998).
- [34] M. Lebugle, M. Gräfe, R. Heilmann, A. Perez-Leija, S. Nolte, and A. Szameit, *Experimental observation of N00N state Bloch oscillations*, *Nat. Commun.* **6**, 8273 (2015).
- [35] J. G. Muga, J. P. Palao, B. Navarro, and I. L. Egusquiza, *Complex absorbing potentials*, *Phys. Rep.* **395**, 357 (2004).

SUPPLEMENTAL MATERIAL

In order to illustrate with examples the versatility of the A-R photonic simulator, we show numerical calculations of each genuine physical situation developed in the manuscript.

Dynamical Parameters

Consider the oscillatory time dependence of the propagation constant, β , for the single variable A-R equation, Eq. (1) in the manuscript. We numerically simulate this system for a lattice of $N = 6$ waveguides, $\beta = 1$, $\kappa = \sqrt{7}$, $\epsilon = 1$ and $\omega = 2$, see Fig. 5. We have selected these parameters to show the existence of resonant solutions, in which a high amount of light gets trapped in the chip. Notice that, although a high population is achieved in the stationary state, the theoretical error is still small.

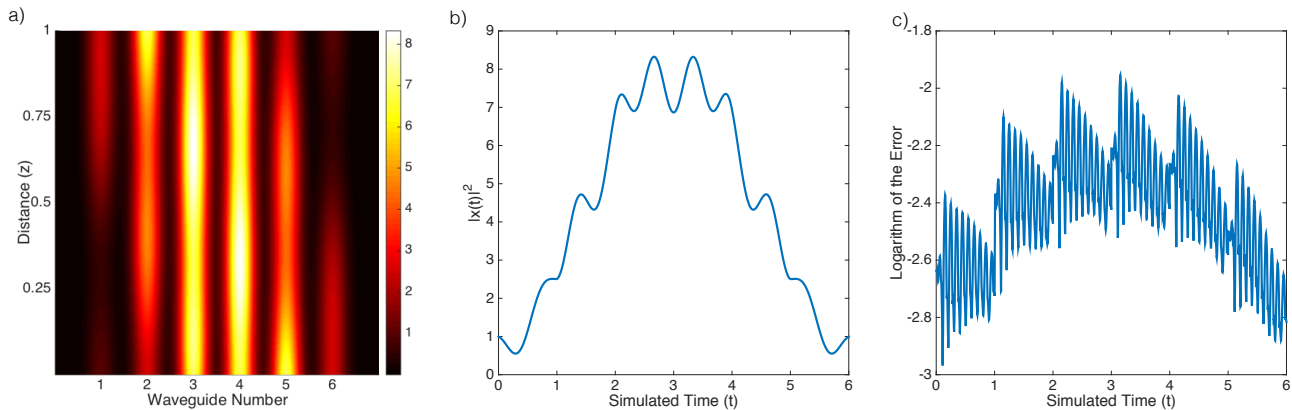


FIG. 5: Numerical Simulation of Eq. (1) with $N = 6$, $\beta = 1$, $\epsilon = 1$, $\kappa = \sqrt{7}$, $\omega = 2$. (a) Intensity in the stationary state in the waveguides array. (b) Modulus square of the solution as a function of time. (c) Decimal Logarithm of the error of the simulation with respect to the solution of the A-R equation.

Systems of Equations

In Fig. 6, we plot a numerical simulation of the array proposed to simulate systems of A-R equations given by Eq. (3). The dynamical parameters are $N = 5$, $\beta_x = 1$, $\beta_y = 2$, $\kappa_x = 3$, $\kappa_y = 1$, $q = 1$, $d = 1$ and $\tau = 1$ for an initial state $|\psi(0)\rangle = |0\rangle$. The theoretical error is smaller than 10^{-2} for the complete time evolution. We have selected these parameters to show that highly asymmetric solutions are also possible for time independent equations even with the limitation induced by the physical constrains in the coupling constants κ .

Multiple Delays

Eq. (6) in the manuscript describes the evolution of a system driven by two feedback and two forward terms. See Fig. 7 for a numerical simulation of this equation with $N = 5$, $\beta = 1$, $\kappa = 5$ and $\tau = 1$.

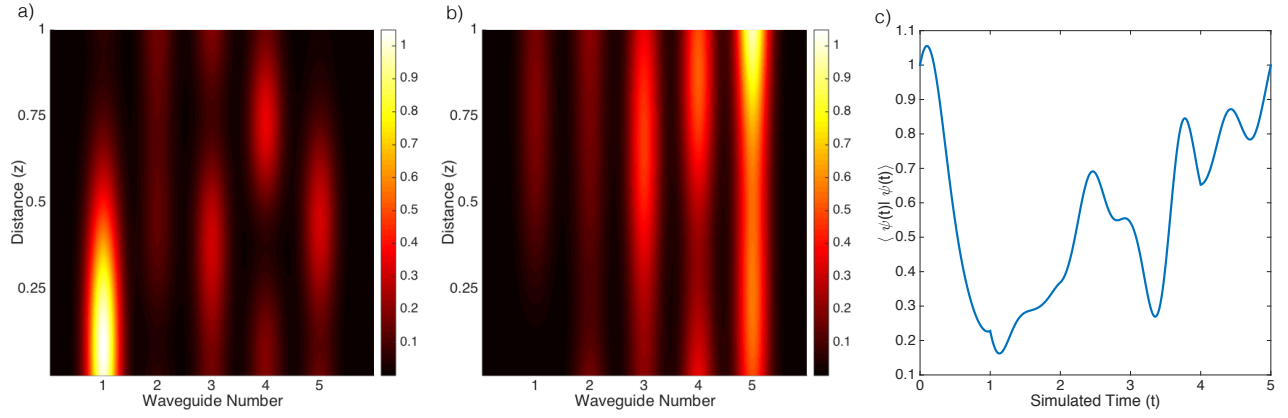


FIG. 6: Numerical simulation of Eq. (3) with $N = 5$, $\beta_x = 1$, $\beta_y = 2$, $\kappa_x = 3$, $\kappa_y = 1$, $q = 1$, $d = 1$, $\tau = 1$ for the initial state $|\psi(0)\rangle = |0\rangle$. (a) Waveguide intensity in the x plane corresponding to the first component of the qubit. (b) Waveguide intensity in the y plane corresponding to the second component of the qubit. (c) Modulus square of the quantum state as a function of time.

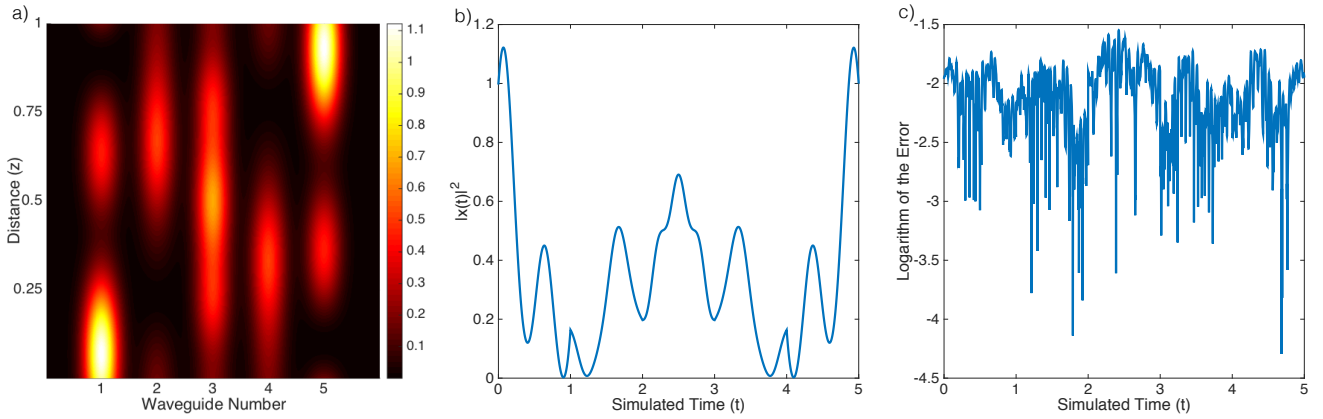


FIG. 7: Numerical simulation of Eq. (6) with $N = 5$, $\beta = 1$, $\kappa = 5$ and $\tau = 1$. (a) Intensity in the stationary state in the waveguide array. (b) Modulus square of the solution as a function of time. (c) Decimal logarithm of the simulation error with respect to the solution of the A-R equation.